Volume 18, No 1 | International Journal of Radiation Research, January 2020

Estimation of the visual system complication probability on children with Medulloblastoma after Craniospinal irradiation with three-dimensional conformal radiotherapy

P. Shoa[1], I. Abedi[1,2], M.B. Tavakoli[1*], A.R. Amouheidari[2], K. Jabbari[1]

[1]*Department of Medical Physics, School of Medicine, Isfahan University of Medical Sciences, Isfahan, Iran*
[2]*Department of Radiation-Oncology, Isfahan Milad Hospital, Isfahan, Iran*

► ***Original article***

Corresponding authors:
Mohammad B. Tavakoli, PhD.,
Fax: *+ 98 313 668 8597*
E-mail:
mohamadbtavakoli@gmail.com

Revised: April 2019
Accepted: May 2019

Int. J. Radiat. Res., January 2020; 18(1): 117-123

DOI: 10.18869/acadpub.ijrr.18.1.117

ABSTRACT

Background: The use of radiation therapy for medulloblastoma can affect children's visual system. We estimated children's visual system complication probability in the craniospinal irradiation (CSI) technique with three-dimensional conformal radiotherapy (3D-CRT). ***Materials and Methods:*** CSI of fifteen medulloblastoma patients and a phantom were planned with 6 MV photon beams and 23.4 Gy prescribed dose. The doses of lenses were measured using thermoluminescence dosimeters (TLD). The delivered doses and complication probabilities were calculated based on the equivalent uniform dose (EUD) model to each contoured organ, including the bilateral lenses, optic nerves, retinas and optic chiasm. ***Results:*** The received dose for each organ was less than the tolerance value ($p<0.001$), except for the eye lens. The normal tissue complication probability (NTCP) values for all of the organs at risk (OAR) were found insignificant. The discrepancies of calculated and measured doses for the right and left lenses were 6.35% and 6.23% ($p<0.001$), respectively. ***Conclusion:*** The results of this study showed based on the International Commission on Radiological Protection (ICRP) publication 118 that children with medulloblastoma cancer treated with CSI with 3D-CRT method are susceptible to cataract complication.

Keywords: *Visual System Complication Probability, Medulloblastoma, Craniospinal Irradiation, Three-dimensional conformal radiotherapy.*

INTRODUCTION

Medulloblastoma is a primitive neuroectodermal tumor (PNET) and originates from the cerebellum or fourth ventricle. It is one of the most common tumors of the central nervous system (CNS) in children [1, 2]. The main treatments for such patients are craniospinal irradiation (CSI) and chemotherapy. CSI technique consists of a pair of lateral parallel opposed fields to treat the brain and one or two posterior fields to the spinal axis with a boost consisting of four different gantry angle fields, two opposing fields of the posterior fossa [3, 4]. Three-dimensional conformal radiotherapy (3D-CRT) is a standard technique for treating this cancer nowadays [4].

The aim of radiation therapy is to deliver prescribed dose to the tumor [5]. It has been shown that head and neck external radiotherapy causes inevitably radiation doses delivered to healthy tissues and organs at risk (OAR), due to primary and stray beams. Brain radiotherapy has been reported to produce late effects in the visual system such as visual impairment, cataract, radiation retinopathy and optic neuropathy [2, 6-10]. It can be avoided blindness due to lens opacity by surgery, but there is no proven effective treatment for blindness due to retina, optic nerve and optic chiasm injury [6, 11].

[DOI: 10.18869/acadpub.ijrr.18.1.117]

Several biological models are existed predicting the risk of late normal tissue complication based on the physical dose distribution and irradiated volume. In recent years, many treatment plans have evaluated and ranked using radiobiological models in term of expected late occurring deterministic sequel [12-14].

Studies of complication probability for medulloblastoma patients were mostly focused on the intellectual problems and few studies have been done regarding the visual system complications, according to increasing the survival rate in recent decades [15-17]. Brodin et. al. estimated insignificant incidence of complication for blindness rate due to optic nerve injury following 23.4 Gy CSI in photon 3D-CRT technique, using the linear function model [4]. In their study, it was not calculated normal tissue complication probabilities (NTCP) for other parts of the visual system. None of the previous studies estimated complication probability for the child's visual system completely, using the equivalent uniform dose (EUD) model. The aim of this clinical investigation was to estimate the cataract, optic neuropathy and retinopathy due to CSI, using the evaluation of the radiobiological competence of the EUD model.

MATERIALS AND METHODS

Contouring and Treatment Planning

It was studied fifteen pediatric medulloblastoma patients with standard risks (10 males, 5 females), with a median age of 7.8±3.1 (4-13 years), who underwent CSI in the supine positions. The current study was approved by the Isfahan University of Medical Sciences Review-board of Research Ethics (approved April 9, 2019; Registration number IR.MUI.MED.REC.1398.003).

Treatment plans were generated using computed tomography (CT) images on Prowess Panther treatment planning system (TPS) version 5.5. A radiation oncologist contoured the clinical target volume (CTV) including the whole brain and spinal cord, as well as OARs including the right and left optic nerves, lenses, retinas, eyeballs, lacrimal glands, parotid, lungs, kidneys, cochleas, esophagus, larynx, heart, brain stem, thyroid gland and optic chiasm.

In this study, the dose of right and left optic nerves, lenses, retinas and optic chiasm were evaluated. The whole posterior fossa is typically contoured as the site of primary tumor. For possible positioning errors, the planning target volume (PTV) and boost plans were created by expanding the whole brain, spinal cord (the CTV) and posterior fossa by 10, 5 and 10 mm, respectively, in all directions. The CTV also included the cribriform plate. The OARs dose constraints were based on the International Commission on Radiological Protection (ICRP) publication 118, the quantitative analysis of normal tissue effects in the clinic (QUANTEC), and Emami *et al.* [18-20].

CSI included a pair of lateral parallel opposed fields to treat the whole brain and one posterior field to the spinal axis. A 2-3 mm skin gap was left between the cranial and spinal fields. Based on patient's head position, collimator of the cranial fields was rotated to match with the superior border of the spinal field to uniform the treatment of the entire craniospinal target volume. The lower border of the cranial fields was placed at C_4-C_6 to decrease the risk of developing hypothyroidism. The cranial fields didn't pass transversely the shoulders. Multileaf collimators (MLC) were used to shape the fields, and to protect the lenses and eyeballs from primary photon beams, except for partial of the PTV. Oral cavity was shielded. The posterior fossa was boosted with four oblique fields after completion of CSI [3, 4, 21].

The plans for the patients were based on 23.4 Gy to the PTV and 54 Gy to the whole posterior fossa, using a 6 MV siemens Artiste linear accelerator and an isocentric technique delivering 1.8 Gy fractions daily and 5 fractions in a week. Each plan was normalized to its isocenter [3]. According to ICRU Report No. 50, the entire PTV received at least 95% of the prescription dose [22]. In order to study the patient's treatment plan, CSI plan was composed with boost plan and a composite plan was created. The OARs doses were derived from

[DOI: 10.18869/acadpub.ijrr.18.1.117]

DVH.

Phantom Dosimetry

TPS calculations for eye lenses may not be accurate enough because they are located under shielding MLCs [23]. Thus, it was used a pediatric Perspex phantom to measure the eye lens doses accurately. Treatment plans were generated using 3 mm thick CT images in the supine position and it was embedded a cubic lithium fluoride (LiF: Mg,Ti) thermoluminescence dosimeter (TLD) chip (3 mm×3 mm×1 mm) in each hole of phantom instead of the lenses. The TLDs were calibrated by 6 MV photon beams. At first, it was measured each TLD's individual calibration factor (ICF) with 100 cGy dose. Then, in order to determine batch calibration factor (BCF), the dosimeters were divided into seven groups. A group wasn't exposed, rather used as control and others were irradiated with 30, 60, 90, 120, 150 and 180 cGy doses [24, 25]. It was used a SOLARO-2A Model TLD reader (NE company) to measure dose absorbed by the TLDs. Then the phantom was irradiated in the similar therapeutic position. TLD measurements were obtained three times.

EUD Mathematical Model

Several models for prediction of NTCP are recommended [12, 26-28]. The NTCP estimates the probability of a complication after uniform dose of a partial volume of organ or tissue. For this purpose, the EUD algorithm is used. The EUD is the uniform dose, if delivered over the same number of fractions to the target volume as the non-uniform dose distribution of interest that gives the same radiobiological effect. In order to estimate radiation induced visual system complication probability, EUD model suggested by Niemierko *et al.* was used in this study and normal tissue tolerance data by Emami *et al.* [12, 13, 29]. The EUD is defined as equation (1):

$$EUD = \left(\sum_{i=1} viDi^{a}\right)^{\frac{1}{a}} \quad (1)$$

Where, v_i is a parameter with no unit, expressing the i^{th} partial volume of organ that receives D_i dose in Gy. In addition, *a* is a unitless parameter which is specific for each organ and describes the volume effect. The EUD is substituted in the following equation (2) to calculate the NTCP:

$$NTCP = \frac{1}{1+\left(\frac{TD_{50}}{EUD}\right)^{4\gamma_{50}}} \quad (2)$$

TD_{50} is tolerance dose for the normal tissue at 50% NTCP after radiotherapy [29]. γ_{50} is a model parameter with no unit that is specific for each organ and explains the slope of the dose-response curve. The value of visual system radiobiological parameters was compiled by Niemierko *et al.* [12, 30]. According to The TPS capability to show the NTCP results with two decimal numbers, the NTCP (%) values were calculated to five decimal places.

Statistical analysis

The one sample t-test was used to compare the calculated OARs dose results with tolerance data. This test was also used to evaluate mean differences between measured and calculated values. There was a statistically significant difference ($p<0.05$). Statistical analysis was performed by SPSS software version 22.0.

RESULTS

An example of the dose distribution of brain PTV was shown in figure 1. As shown, all the treatment region was covered with the 95% prescribed dose and the optic nerves, optic chiasm and retinas were entirely within the treatment region. Although the lenses were shielded by the sufficient MLCs, they received a dose due to the proximity of the treatment region and photon decreasing beyond the target slowly. Table 1 summarizes the mean calculated doses, the measured doses with standard deviation (SD) values and the differences between the values for the right and left lenses. The results of other treatment characteristics of studied patients with SD values by the TPS are presented in table 2. For all the studied patients, a significant difference was seen in the OAR received dose and threshold dose ($p<0.001$).

[DOI: 10.18869/acadpub.ijrr.18.1.117]

Table 1. Measured and calculated radiation dose to the eye lens.

	Calculated dose (cGy) ± SD	Range	Measured dose (cGy) ± SD	Range	Measured vs. calculated doses	
					%	P value
Right lens	533.05 ± 149.78	223.5-727.1	569.22 ± 1.75	567.16-571.43	6.35	<0.001
Left lens	521.87 ± 152.95	204.6-695.3	556.52 ± 2.35	553.81-559.55	6.23	<0.001

Table 2. Treatment characteristics of the studied patients.

Characteristic	Quality ± SD	Range
Right lens		
EUD (cGy)	605.06 ± 172.39	223.9-832
NTCP (%)	1.76 ± 1.21	0.02-4.37
Left lens		
EUD (cGy)	583.22 ± 178.42	214.9-779.2
NTCP (%)	1.59 ± 1.06	0.02-3.39
Right optic nerve		
D_{max} (cGy)	3228.71 ± 108.45	3030.1-3481.9
EUD (cGy)	2947.81 ± 126.79	2801.5-3252.8
NTCP (%)	0.0086 ± 0.0053	0.00411-0.0247
Left optic nerve		
D_{max} (cGy)	3137.5 ± 87.61	3015.5-3288
EUD (cGy)	2898.06 ± 93.32	2794.5-3080.3
NTCP (%)	0.0066 ± 0.00288	0.00398-0.0128
Optic chiasm		
D_{max} (cGy)	5084.08 ± 115.42	4831.5-5261.6
EUD (cGy)	4749.96 ± 116.32	4535.1-4946.9
NTCP (%)	2.35 ± 0.67	1.313-3.639
Right retina		
D_{max} (cGy)	2687.83 ± 136.76	2493.7-2997.4
EUD (cGy)	2519.89 ± 80.1	2381.2-2662.5
NTCP (%)	0.0524 ± 0.013	0.03243-0.0792
Left retina		
D_{max} (cGy)	2609.12 ± 102.32	2455.8-2786.4
EUD (cGy)	2521.45 ± 81.93	2411.2-2672.9
NTCP (%)	0.0524 ± 0.0145	0.03584-0.0817

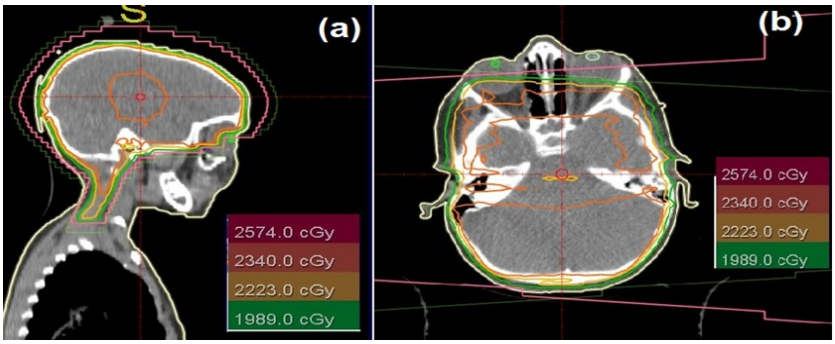

Figure 1. Isodose distributions for brain fields in the sagittal **(a)** and axial CT slices **(b)**.

DISCUSSION

The dose received by OARs was calculated using a TPS and TLD. Then the visual system complication probability was estimated using the EUD radiobiological model for standard risk of 15 pediatric medulloblastoma patients treated with photon 3D-CRT.

The TLD measurements showed a significant difference compared to the TPS ($p<0.001$) (table 1). This may have been due to three reasons. First, studies have shown that the TPS's ability to

[DOI: 10.18869/acadpub.ijrr.18.1.117]

calculate a scattered dose is low, so the dose received by the lens is less than its actual value. Second, the small set-up errors due to the dose gradient near the lens area lead to a large difference. Third, previous published reports showed that the small size of the lens affects TPS calculations and can lead to a large discrepancy [23, 31, 32]. The differences in this study were in agreement with the American Association of Physicists in Medicine Radiation Therapy Committee Task Group 53 (AAPM TG-53) and as a consequence of the measured results for the supine position, the TPS calculations can estimate the delivered eye lens dose sufficiently [23, 33]. Similar results have been reported in other studies. Hood *et al.* have measured OARs received doses with 6 MV photon beams, using an anthropomorphic phantom in prone position and reported the lens received dose less than 1 Gy following 4 Gy cranial dose for both the TPS and TLD values [34]. Results in our study are slightly higher than those in their work, because of the boost plan considered in our study. Although the results of this study is not in accordance with the research by Baghani et. al. who reported that, however the mean right and left lens doses of the CSI with 50 cGy and 6 MV photon beams using a Rando phantom in prone position are 34% and 28%, respectively [25]. A significant difference between the two studies may be due to different treatment position and junction adjustment between the cranial and spinal fields.

NTCPs are biological models based on retrospective data collected from the clinical outcomes on organs and the steepness of the dose-response relationship mostly based on normal tissue tolerance values by Emami *et al.* [12, 14]. In 2012, the lens dose tolerance provided by them was refined as low as 0.5 Gy by ICRP publication 118 recommendations and was proved in a long follow-up study for children [16, 20]. On the basis of our analysis, the delivered dose of OARs, except for the lens, were lower than tolerance data with significant differences ($p<0.001$) and the NTCP values of the visual system were not shown remarkable results (table 2). Although, the results of the received dose by lens were about 10 times higher compared to the ICRP (>520 cGy vs. 50 cGy) (table 1), the NTCP value clearly underestimated possible damage to the lens and the calculated cataract probability lacked the confirmation of ICRP result [20]. Therefore, the calculated cataract probability based on published clinical data by Emami *et al.* was misfit with ICRP threshold and the model might be misleading for the lens. It might be safer to focus on the mean dose by the lens instead of NTCP value. In another study, Patel *et al.* found the mean lens received dose about 20 Gy following 23.4 Gy CSI [35]. The high mean dose related to the lens in the previous study was likely depending on using a variety of MLCs adjustment near the lens region. Brodin *et al.* estimated the blindness NTCP value from the optic nerves slightly higher than ours (>3%) because of using different NTCP model (linear function) [4]. In summary, this study suggested for patients had no ocular disease that although 3D-CRT maybe an optimal choice based on sparing of the optic nerves, optic chiasm and retinas, it can't succeed to reduce optimally the mean total dose below the 0.5 Gy threshold level to the lenses and it may be the cause of the incidence of the cataract complication years after exposure.

The important strength of this study was the usage of the pediatric anthropomorphic phantom that provided therapeutic and stray doses for current photon therapy and enabled us to determine the most accurate evaluation of the radiation dose delivered to the OARs. However, this study also had a limitation that is common for this topic. This retrospective review only focused on the TPS results and did not verify treatment delivery of plans. Performing pretreatment image-guided radiation therapy (IGRT) and identifying the eye lens's position would be an important component of the full estimation of cataract complication for CSI due to high dose gradient near the lens region [23]. Future studies should estimate cataract complication based on more patients during long follow-up considering the epidemiological data included cataract risk factors other than radiation exposure in these pediatric patients.

[DOI: 10.18869/acadpub.ijrr.18.1.117]

CONCLUSION

The results of this study showed based on the ICRP publication 118 that children with medulloblastoma cancer treated with CSI with 3D-CRT method are susceptible to cataract complication.

ACKNOWLEDGMENT

The authors acknowledge support for a MSc. degree grand No. 397551 from Isfahan University of Medical Science (IUMS). The authors would like to thank the staff members of the radiation oncology department at the Isfahan Milad hospital, Isfahan, Iran, for their supporting in this work.

Conflicts of interest*: *Declared none.

REFERENCES

1. Bartlett F, Kortmann R, Saran F (2013) Medulloblastoma. *Clinical Oncology,* ***25(1)****: 36-45*.
2. Laprie A, Hu Y, Alapetite C, Carrie C, Habrand J-L, Bolle S, *et al.* (2015) Paediatric brain tumours: a review of radiotherapy, state of the art and challenges for the future regarding protontherapy and carbontherapy. *Cancer/ Radiotherapie,* ***19(8)****: 775-789*.
3. Halperin EC, Brady LW, Perez CA, Wazer DE (2019) Perez & Brady's principles and practice of radiation oncology. Lippincott Williams & Wilkins.
4. Brodin NP, Rosenschöld PMA, Aznar MC, Kiil-Berthelsen A, Vogelius IR, Nilsson P, *et al.* (2011) Radiobiological risk estimates of adverse events and secondary cancer for proton and photon radiation therapy of pediatric medulloblastoma. *Acta oncologica,* ***50(6)****: 806-816*.
5. Kahn F and Gibbons J (2014) Khan's the physics of radiation therapy. Philadelphia, PA: Lippincott Williams and Wilkins.
6. Jeganathan VSE, Wirth A, MacManus MP (2011) Ocular risks from orbital and periorbital radiation therapy: a critical review. *Int J Radiat Oncol Biol Phys,* ***79(3)****: 650-659*.
7. Mayo C, Martel MK, Marks LB, Flickinger J, Nam J, Kirkpatrick J (2010) Radiation dose–volume effects of optic nerves and chiasm. *Int J Radiat Oncol Biol Phys,* ***76(3)****: S28-S35*.
8. Scoccianti S, Detti B, Gadda D, Greto D, Furfaro I, Meacci F, *et al.* (2015) Organs at risk in the brain and their dose-constraints in adults and in children: a radiation oncologist's guide for delineation in everyday practice. *Radiotherapy and Oncology,* ***114(2)****: 230-238*.
9. Whelan KF, Stratton K, Kawashima T, Waterbor JW, Castleberry RP, Stovall M, *et al.* (2010) Ocular late effects in childhood and adolescent cancer survivors: a report from the childhood cancer survivor study. *Pediatric blood & cancer,* ***54(1)****: 103-109*.
10. Zhang R, Howell RM, Giebeler A, Taddei PJ, Mahajan A, Newhauser WD (2013) Comparison of risk of radiogenic second cancer following photon and proton craniospinal irradiation for a pediatric medulloblastoma patient. *Physics in Medicine and Biology,* ***58(4)****: 807-823*.
11. Miralbell R, Cella L, Weber D, Lomax A (2000) Optimizing radiotherapy of orbital and paraorbital tumors: intensity-modulated X-ray beams vs. intensity-modulated proton beams. *Int J Radiat Oncol Biol Phys,* ***47(4)****: 1111-1119*.
12. Gay HA and Niemierko A (2007) A free program for calculating EUD-based NTCP and TCP in external beam radiotherapy. *Physica Medica,* ***23(3-4)****: 115-125*.
13. Niemierko A and Goitein M (1993) Modeling of normal tissue response to radiation: the critical volume model. *Int J Radiat Oncol Biol Phys,* ***25(1)****: 135-145*.
14. Fuss M, Poljanc K, Miller DW, Archambeau JO, Slater JM, Slater JD, *et al.* (2000) Normal tissue complication probability (NTCP) calculations as a means to compare proton and photon plans and evaluation of clinical appropriateness of calculated values. *International Journal of Cancer,* ***90(6)****: 351-358*.
15. Cassidy L, Stirling R, May K, Picton S, Doran R (2000) Ophthalmic complications of childhood medulloblastoma. Medical and Pediatric Oncology: The Official Journal of SIOP—International Society of Pediatric Oncology (Societé Internationale d'Oncologie Pédiatrique), **34(1)**: 43-47.
16. Chodick G, Sigurdson AJ, Kleinerman RA, Sklar CA, Leisenring W, Mertens AC, *et al.* (2016) The risk of cataract among survivors of childhood and adolescent cancer: a report from the childhood cancer survivor study. *Radiation Research,* ***185(4)****: 366-374*.
17. Howell RM, Giebeler A, Koontz-Raisig W, Mahajan A, Etzel CJ, D'Amelio AM, *et al.* (2012) Comparison of therapeutic dosimetric data from passively scattered proton and photon craniospinal irradiations for medulloblastoma. *Radiation Oncology,* ***7(1)****: 116-127*.
18. Emami B (2013) Tolerance of normal tissue to therapeutic radiation. *Reports of Radiotherapy and Oncology,* ***1(1)***: *35-48.*
19. Marks LB, Yorke ED, Jackson A, Ten Haken RK, Constine LS, Eisbruch A, *et al.* (2010) Use of normal tissue complication probability models in the clinic. *Int J Radiat Oncol Biol Phys,* 76(3): S10-S19.
20. Stewart F, Akleyev A, Hauer-Jensen M, Hendry J, Kleiman N, Macvittie T, *et al.* (2012) ICRP publication 118: ICRP statement on tissue reactions and early and late effects of radiation in normal tissues and organs–threshold doses for tissue reactions in a radiation protection context. *Annals of the ICRP,* ***41(1)****: 1-322.*
21. Tongwan D, Peerawong T, Oonsiri S, Shotelersuk K (2010) Craniospinal irradiation in the supine position: a

[DOI: 10.18869/acadpub.ijrr.18.1.117]

dosimetric analysis. *Asian Biomed,* ***3(6)****: 699-708*.
22. Parker W, Patrocinio H, Podgorsak MB, Podgorsak EB (2005) Radiation oncology physics: A handbook for teachers and students. 219 p.
23. Wang X, Li G, Zhao J, Song Y, Xiao J, Bai S (2019) Verification of eye lens dose in IMRT by MOSFET measurement. *Medical Dosimetry.* ***44(2):*** *107-110.*
24. Kry SF, Titt U, Pönisch F, Followill D, Vassiliev ON, Allen White R, *et. al.* (2006) A Monte Carlo model for calculating out-of-field dose from a Varian beam. *Medical Physics,* ***33 (11)****: 4405-4413*.
25. Baghani H, Aghamiri S, Gharaati H, Mahdavi S, Daghigh Hosseini S (2011) Comparing the results of 3D treatment planning and practical dosimetry in craniospinal radiotherapy using Rando phantom. *Iran J Radiat Res,* ***9(3)****: 151-158*.
26. Bakhshandeh M, Hashemi B, Mahdavi SRM, Nikoofar A, Vasheghani M, Kazemnejad A (2013) Normal tissue complication probability modeling of radiation-induced hypothyroidism after head-and-neck radiation therapy. *Int J Radiat Oncol Biol Phys,* ***85(2)****: 514-521*.
27. Kehwar T (2005) Analytical approach to estimate normal tissue complication probability using best fit of normal tissue tolerance doses into the NTCP equation of the linear quadratic model. *Journal of cancer research and therapeutics,* ***1(3):*** *168-179.*
28. Lyman JT (1985) Complication probability as assessed from dose-volume histograms. *Radiation Research,* ***104(2s)****: S13 -S19*.
29. Emami B, Lyman J, Brown A, Cola L, Goitein M, Munzenrider J, *et al.* (1991) Tolerance of normal tissue to therapeutic irradiation. *Int J Radiat Oncol Biol Phys,* ***21(1)****: 109-122*.
30. Oinam AS, Singh L, Shukla A, Ghoshal S, Kapoor R, Sharma SC (2011) Dose volume histogram analysis and comparison of different radiobiological models using in-house developed software. J*ournal of medical physics/Association of Medical Physicists of India,* ***36(4)****: 220-229*.
31. Howell RM, Scarboro SB, Taddei PJ, Krishnan S, Kry SF, Newhauser WD (2010) Methodology for determining doses to in-field, out-of-field and partially in-field organs for late effects studies in photon radiotherapy. *Physics in Medicine & Biology,* ***55(23)****: 7009-7023*.
32. Ebert M, Haworth A, Kearvell R, Hooton B, Hug B, Spry N, *et al.* (2010) Comparison of DVH data from multiple radiotherapy treatment planning systems. *Physics in Medicine & Biology,* ***55(11)****: N337-N346.*
33. Fraass B, Doppke K, Hunt M, Kutcher G, Starkschall G, Stern R, *et al.* (1998) American Association of Physicists in Medicine Radiation Therapy Committee Task Group 53: quality assurance for clinical radiotherapy treatment planning. *Medical physics,* ***25(10)****: 1773-1829*.
34. Hood C, Kron T, Hamilton C, Callan S, Howlett S, Alvaro F, *et al.* (2005) Correlation of 3D-planned and measured dosimetry of photon and electron craniospinal radiation in a pediatric anthropomorphic phantom. *Radiotherapy and Oncology,* ***77(1)****: 111-116*.
35. Patel S, Drodge S, Jacques A, Warkentin H, Powell K, Chafe S (2015) A Comparative Planning Analysis and Integral Dose of Volumetric Modulated Arc Therapy, Helical Tomotherapy, and Three-dimensional Conformal Craniospinal Irradiation for Pediatric Medulloblastoma. *Journal of Medical Imaging and Radiation Sciences,* ***46(2)****: 134-140*.

[DOI: 10.18869/acadpub.ijrr.18.1.117]